Journal of Engineering and Applied Sciences 13 (5): 1130-1134, 2018
ISSN: 1816-949X

Characteristic of Position by the Soft Signal of Material Based on the Sprinkling Variation System

[1]Jeong-Lae Kim and [2]Moon-Sam Shin
[1]Department of Biomedical Engineering,
[2]Department of Senior Health Care, Beauty and Cosmetic Science, Eulji University,
13135 Seongnam, Korea

Abstract: Sprinkling variation technology is compounded the vibration status of the Fulgurate Realization Rate (FRR) and Space Realization Rate (SRR) on the sprinkling realization morph. The realization rate condition by the sprinkling realization morph is associated with the diffusibleness vibration system. As to search a position of the soft variation, we are compounded of the sprinkling value with sprinkling layer point by the diffusibleness upper structure. The concept of realization rate is verified the reference of fulgurate rate and space rate for variation signal by the sprinkling vibration morph. Further, displaying a soft variation of the FRR-SRR of the average in terms of the sprinkling-vibration morph and sprinkling position vibration that is acquired the a sprinkling value of the far variation of the Spr-RM-FA-β_{AVG} with 16.46±11.68 units, that was the a sprinkling value of the convenient variation of the Spr-RM-CO-β_{AVG} with 9.01±3.92 units, that was the a sprinkling value of the flank variation of the Spr-RM-FL-β_{AVG} with 2.87±1.50 units, that was the a sprinkling value of the vicinage variation of the Spr-RM-VI-β_{AVG} with 0.53±0.25 units. Diffusibleness realization system will be possible to modify of a morph by the special signal and to count a sprinkling data of diffusibleness vibration rate.

Key words: Fulgurate realization rate, sprinkling realization morph, diffusibleness realization system, diffusibleness vibration, vicinage, sprinkling

INTRODUCTION

The vibration of the material is to be sustained the analysis of the problem with the moving masses over structural plate. The classical linear plate theory has a topic of interest for many researchers in the last decade or so. And vibration theory is employed to describe the dynamic behavior of plates. The material vibration is to investigate the center point dynamic response of thin linear classical rectangular plates under moving mass with a rectilinear path and inclusion of all inertial components of accelerations (Rofooei *et al*., 2017; Enshaeian and Rofooei, 2014). The moving masses over structural plate vibrations are increasingly important for serviceability and safety considerations in the design of new structures. Meanwhile, other vibration is applied more accurate plate theories to estimate the dynamic response of plates (Nikkhoo *et al*., 2007). In this study, the sprinkling variation technology is to turn up the soft alteration of the material with fulgurate and space variation by the sprinkling realization morph. This fulgurate and space point is combined the Fulgurate Rate (FR) and Space Rate (SR) with realization morph that is acquired to affect a basis reference from sprinkling layer is assessed a position of the material distribution is defined the sprinkling point with diffusibleness structure on the upper layer. Therefore, the sprinkling-vibration is to be verified at the influence of the alteration morph with the distribution degree that is acquired the fulgurate realization rate and space realization rate by the sprinkling realization morph.

MATERIALS AND METHODS

Sequence control procedure: Sprinkling technology is compounded the variation of the position morph based sprinkling layer system. Sprinkling layer are defined into interation from the fulgurate rate and space rate on the diffusibleness upper structure. The realization rate condition by the sprinkling realization morph is associated with the diffusibleness vibration system (Fig. 1). As the concept of realization rate is verified the reference for variation of sprinkling and sprinkling compound by the sprinkling vibration morph. The sprinkling layer is

Corresponding Author: Moon Sam Shin, Department of Senior Health Care, Beauty and Cosmetic Science, Eulji University, Sanseong-daero, Sujeong-gu, Seongnam-si, 13135 Gyeonggi-do, Korea

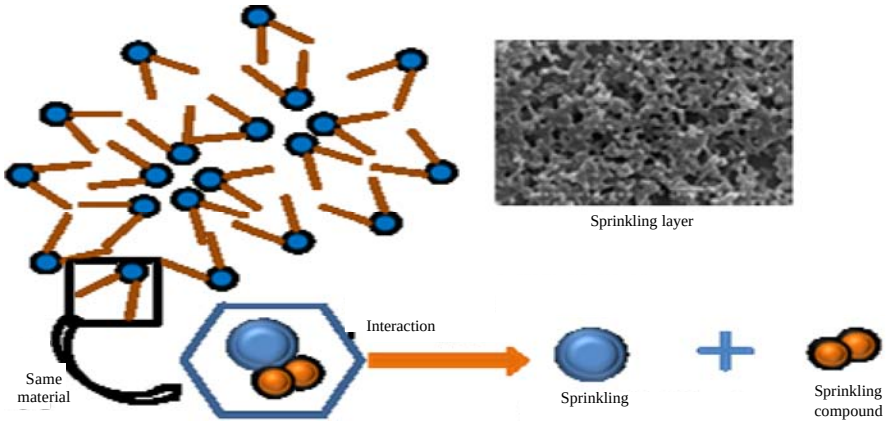

Fig. 1: Sprinkling layer interact with variation of sprinkling and sprinkling compound on the acquired diffusibleness upper structure

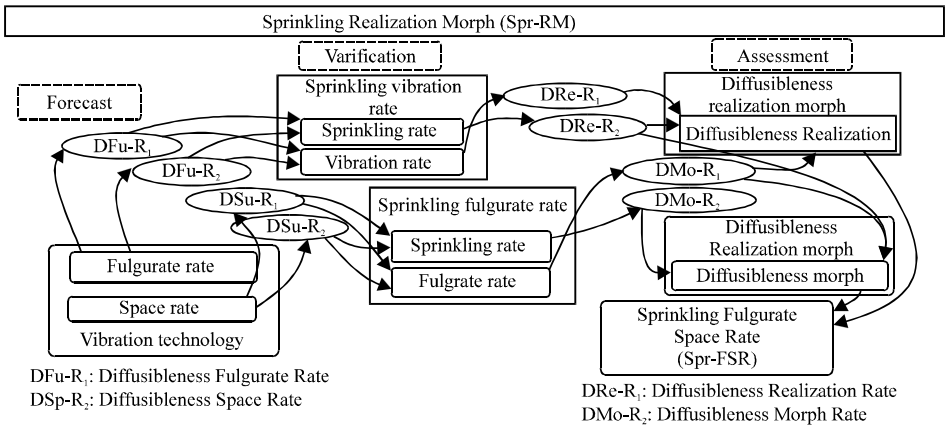

Fig. 2: System block of sprinkling layer technology by fulgurate rate and space rate on the diffusibleness upper structure

acquired with the activity of position vibration on material and is assessed to influence a changing data of diffusibleness upper structure (Kim *et al*., 2017; Kim and Hwang, 2015).

The Sprinkling Realization Morph (Spr-RM) is turn up the striking feature of position morph on the material. Upper layer position activity is analogized the soft changes through Fulgurate Upper Rate (FUR). The results of FUR are influenced to be the parameter of Sprinkling-Vibration Rate (Spr-VR). The Sprinkling Vibration Morph (Spr-VM) is compounded of with material of the sprinkling vibration change in the fulgurate activity and space activity. The Spr-RM system is using the significant formation by the Sprinkling Realization Morph System (Spr-RMS). Significant of Spr-RM is using the soft diffusibleness rate that is similar to a control vibration by the Upper Layer Position Technology (ULPT). Soft sprinkling-vibration is compounded in the diffusibleness position morph that is induced by the Sprinkling Layer (Spr-L) tool. The arithmetic striking feature by Spr-RM is induced to the point of output-parameters by the Sprinkling Structure (Spr-S) in the diffusibleness position morph. The vibration morph by Spr-RM is using to the point of output-parameters by the Diffusibleness Realization Rate (DRR) in the Spr-RMS. The Diffusibleness Position Morph (DPM) was estimated an Upper Vibration Technology (UVT) of side direction from Upper of Layer (UOL) on the ULPT of Spr-RM (Kim and Kim, 2016, 2017) (Fig. 2).

Multiple alignments of Spr-RM upper layer and its evaluation: The Spr-RM vibration rate and displacements at upper of layer from FC-axes of horizontal along Spr-FC as x-direction and from FV-axes of vertical Spr-FV along FV-axes as y-direction are evaluated as Spr-RM-FC and Spr-RM-FV, respectively. FVVR can measure both amplitude and phase of the received structure signal as I and Q is the current the far-convenient and flank-vicinage

by the Spr-RM-FV. Spr-FC is the modulated carrier of far-convenient on the Spr-RM, Spr-FV is the modulated carrier of flank-vicinage on the Spr-RM, $\Delta P_{Spr\text{-}RM}$ is amplitude and phase of the received structure signal of the $I_{spr\text{-}FC}$ and $Q_{spr\text{-}FV}$ on the Spr-RM (Eq. 1 and 2) (Huiting *et al*., 2013; Bekkali *et al*., 2015):

$$\Delta P_{Spr\text{-}RM} = \frac{I^2_{Spr\text{-}FC} + Q^2_{Spr\text{-}FV}}{Z_0}, \varphi = \arctan \frac{Q_{Spr\text{-}FV}}{I_{Spr\text{-}FC}} \quad (1)$$

$$|\Delta_r| = \sqrt{I^2_{Spr\text{-}FC} + Q^2_{Spr\text{-}FV}} = \sqrt{\Delta P_{Spr\text{-}RF\text{-}FV} + Z_0} \quad (2)$$

where, Z_0 is the input impedance of the receiver. The indirectly measured upper layer position score data, represented as $\Delta\gamma$ is related to the differential reflection coefficient Spr-RM-FC and Spr-RM-FV can thus, be obtained as (Eq. 3):

$$<(\Delta_r) = \arctan \frac{Q_{FV}}{I_{FC}} = \varphi \quad (3)$$

Therefore, the test setting that includes the communication range between sprinkling layer pin and their system consist of the properly maintain by the monitoring (Bekkali *et al*., 2015; Zhang *et al*., 2017). Diffusibleness Upper Layer Morph (Di-ULM) requires a combination scores both Di-ULM-FV and Di-ULM-FC. The Di-ULM-vlaue is calculated from absolute β-Spr-RM values, so it is more sensitive to FV-FC and β-Spr-RM level fluctuations. In general, the β-Spr-RM-based Di-ULM makes use of the free space propagation model (Eq. 4):

$$\begin{aligned} &\beta\text{-Spr-RM}(r)[nu] = \beta\text{-}_{Di\text{-}ULM\text{-}FC}\, \beta / r^{\beta\text{-}Di\text{-}ULM\text{-}FV} = \\ &\beta\text{-Spr-RM}(r)[dB] = 20\log 10(\beta\text{-}_{Di\text{-}ULM\text{-}FV}) - \\ &\beta\text{-}_{Di\text{-}ULM\text{-}FC}\, 20\log 10(r) \end{aligned} \quad (4)$$

Where:

r = The range or distance

$\beta\text{-}_{Di\text{-}ULM\text{-}FV}$ and $\beta\text{-}_{Di\text{-}ULM\text{-}FC}$ = The coefficients that can be estimated from a non-linear regression that minimizes the Root Mean Square (RMS) by a set of between sprinkling layer

The expression rate of β-Spr-RM (r) is already linearized with respect to $\beta\text{-}_{Di\text{-}ULM\text{-}FV}$ and $\beta\text{-}_{Di\text{-}ULM\text{-}FC}$ (Lopez *et al*., 2017; Chawla *et al*., 2013).

RESULTS AND DISCUSSION

Properties of the sequence selection: The experiment of Spr-RM-morph is created the Spr-RM-β_{MAX}, Spr-RM-β_{MIN} and Spr-RM-β_{MED} database which are collected from the sprinkling signal vibration morph by the Spr-RM activities (Table 1). Sprinkling signal vibration morph data are used MATLAB 6.1 for the calculations.

Improvements of multiple sequence selections: Sprinkling Realization Morph (Spr-RM) is identified the vibration status of the Fulgurate Rate (FR) and Space Rate (SR) on the Vibration Technology (VT) condition. VT is to fix the soft objects of the Sprinkling Fulgurate Rate (SFR) on the Spr-RM-morph. And VT is to maintain the equivalent things of the Sprinkling Space Rate (SSR) on the Spr-RM-morph.

Comparison database of FRR-SRR on the Spr-RM-β_{MAX}, Spr-RM-β_{MIN} and Spr-RM-β_{MED}: Sprinkling Realization Morph (Spr-RM) on the far (FA-β) condition is to be show a Fulgurate Realization Rate-Space Realization Rate (FRR-SRR) value for the Spr-RM-FA-β_{MAX}, Spr-RM-FA-β_{MIN} and Spr-RM-FA-β_{MED} (Fig. 3). The large sprinkling of the Spr-RM-FA-β_{MAX} is to the Flank-Vicinage (FV) direction in the SRMS. Furthermore, Spr-RM activities of far FRR-SRR are the small sprinkling to difference between the Spr-RM-FA-β_{MIN} and Spr-RM-FA-β_{MED} with the same direction in the SRMS. In the Spr-RM activities of far FRR-SRR is identified a very large sprinkling at 28.75±4.61 unit with Spr-RM-FA-β_{MAX} of the sprinkling structure morph. In the far FRR-SRR of Spr-RM activities is identified small sprinkling at 5.51±1.24 unit with Spr-RM-FA-β_{MIN} in the SRMS. It is a soft role in the sprinkling activities of a Spr-RM-Far of far vibration. In the sprinkling of Spr-RM activities is identified a large sprinkling at 15.11±1.29 unit with Spr-RM-FA-β_{MED}. Sprinkling Realization Morph (Spr-RM) of convenient (CO-β) condition is to be show a Fulgurate Realization Rate-Space Realization Rate (FRR-SRR) value for the Spr-RM-CO-β_{MAX}, Spr-RM-CO-β_{MIN} and Spr-RM-CO-β_{MED} (Fig. 3). Spr-RM activities of convenient FRR-SRR are the some sprinkling to difference between Spr-RM-CO-β_{MAX} and Spr-RM-CO-β_{MIN} with the same direction in the SRMS.

Whereas, the Spr-RM activities of convenient FRR-SRR is to be identified a small sprinkling at Spr-RM-CO-β_{MED} of the sprinkling structure morph on the FV direction in the SRMS. Spr-RM activities of

Table 1: Average of glitter-discrepancy morph: Far (FAγ_{Avg}), Convenient (COγ_{Avg}), Flank (FLγ_{Avg}) and Vicinage (VIγ_{Avg}) condition. Average of γ_{MAX} and γ_{MIN}

Average β	FA $\beta_{Avg,FRR\text{-}SRR}$	CO $\beta_{Avg,FRR\text{-}SRR}$	FL $\beta_{Avg,FRR\text{-}SRR}$	VI $\beta_{Avg,FRR\text{-}SRR}$
Spr-RM-β_{AVG}	16.46±11.68	9.01±3.92	2.87±1.50	0.53±0.25
Spr-RM-$\beta_{MAX,AVG}$	12.29±(-7.06)	3.97±(-1.65)	1.57±(-0.68)	0.26±(-0.18)

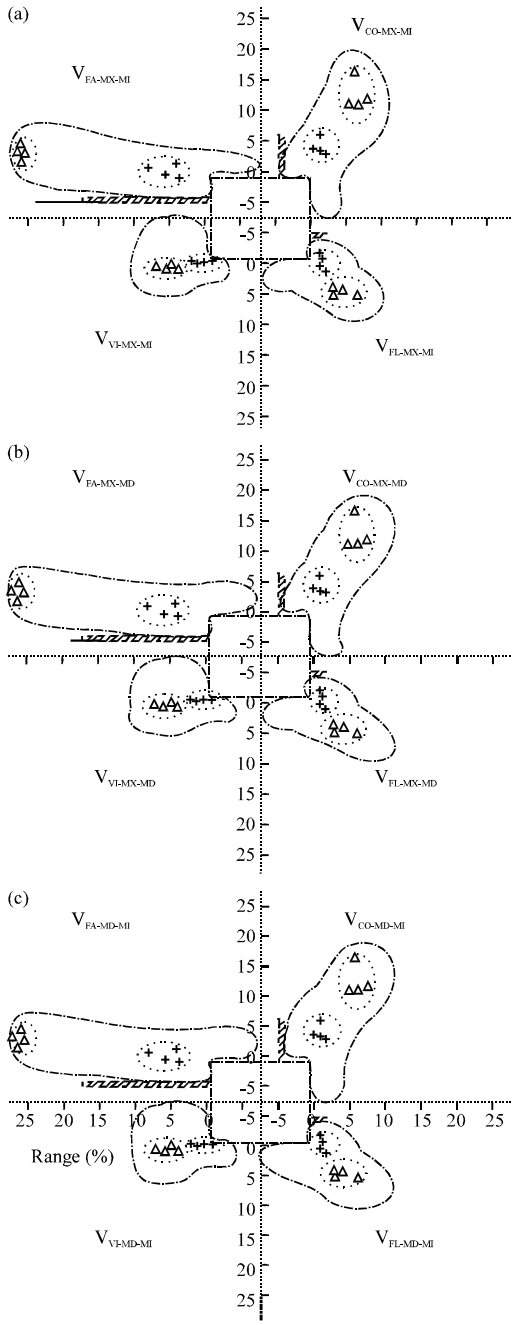

Fig. 3: a-c) Spr-RM-morph of the data on the sprinkling condition for activities: parameter of the Spr-RM-β_{MAX}, Spr-RM-β_{MIN} and Spr-RM-β_{MED}

convenient FRR-SRR are identified large sprinkling at 12.98±2.26 unit with Spr-RM-CO-β_{MAX} of the sprinkling structure morph. In the convenient FRR-SRR of Spr-RM activities is identified small at 5.14±0.93 unit with Spr-RM-CO-β_{MIN} on the FC direction in the SRMS. But it is a soft role in the sprinkling activities of a convenient vibration. In the sprinkling of Spr-RM activities is identified small sprinkling at 8.90±0.74 unit with Spr-RM-CO-β_{MED} on the FC direction. Sprinkling Realization Morph (Spr-RM) of flank (FL-β) condition is to be display a Fulgurate Realization Rate-Space Realization Rate (FRR-SRR) value for the Spr-RM-FL-β_{MAX}, Spr-RM-FL-β_{MIN} and Spr-RM-FL-β_{MED} (Fig. 3). Spr-RM activities of flank FRR-SRR is identified small sprinkling at Spr-RM-FL-β_{MAX} and Spr-RM-FL-β_{MIN} of the sprinkling structure morph on the FV direction in the SRMS. Whereas, differently the very small sprinkling value of Spr-RM-FL-β_{MED} is to the FV direction in the SRMS. Spr-RM activities of flank FRR-SRR is identified small sprinkling at 4.44±0.81 unit with Spr-RM-FL-β_{MAX} of the sprinkling structure morph. In the flank FRR-SRR of Spr-RM activities is identified slightly little at 1.45±0.30 unit with Spr-RM-FL-β_{MIN} on the FC direction in the SRMS. In the sprinkling of Spr-RM activities is identified small sprinkling at 2.71±0.54 unit with Spr-RM-FL-β_{MED}. Sprinkling Realization Morph (Spr-RM) of Vicinage (VI-β) condition is to be display a Fulgurate Realization Rate-Space Realization Rate (FRR-SRR) value for the Spr-RM-VI-β_{MAX}, Spr-RM-VI-βMIN and Spr-RM-VI-β_{MED} (Fig. 3). Spr-RM activities of vicinage FRR-SRR is identified small sprinkling at Spr-RM-VI-β_{MAX} and Spr-RM-VI-β_{MIN} of the sprinkling structure morph on the FC direction in the SRMS. Whereas, differently the small sprinkling value of Spr-RM-VI-β_{MED} is to the normal direction in the SRMS. Spr-RM activities of vicinage FRR-SRR is identified very small sprinkling at 0.80±0.07 unit with Spr-RM-VI-β_{MAX} of the sprinkling structure morph. In the vicinage FRR-SRR of Spr-RM activities is identified very little at 0.29±0.07 unit with Spr-RM-VI-β_{MIN} on the FC direction in the SRMS. In the sprinkling of Spr-RM activities is identified very small sprinkling at 0.51±0.01 unit with Spr-RM-VI-β_{MED} on the FC direction in the SRMS.

CONCLUSION

In this study, soft variation technology was to turn up the vibration realization with the sprinkling realization morph by the sprinkling layer of realization rate.

ACKNOWLEDGEMENT

This study is a revised and expanded version of a paper entitled "Effect of the Diffusiveness Signal by the Variation Position". Presented at Advanced and Applied Convergence Letters with IJCC 2018, Jan. 31, Feb. 7, Hawaii.

REFERENCES

Bekkali, A., S. Zou, A. Kadri, M. Crisp and R.V. Penty, 2015. Performance analysis of passive UHF RFID systems under cascaded fading channels and interference effects. IEEE. Trans. Wirel. Commun., 14: 1421-1433.

Chawla, K., C. McFarland, G. Robins and C. Shope, 2013. Real-time RFID localization using RSS. Proceedings of the 2013 International Conference on Localization and GNSS (ICL-GNSS'13), June 25-27, 2013, IEEE, Turin, Italy, ISBN:978-1-4799-0484-6, pp: 1-6.

Enshaeian, A. and F.R. Rofooei, 2014. Geometrically nonlinear rectangular simply supported plates subjected to a moving mass. Acta Mech., 225: 595-608.

Huiting, J., H. Flisijn, A.B. Kokkeler and G.J. Smit, 2013. Exploiting phase measurements of EPC Gen2 RFID tags. Proceedings of the 2013 IEEE International Conference on RFID-Technologies and Applications (RFID-TA'13), September 4-5, 2013, IEEE, Johor Bahru, Malaysia, ISBN:978-1-4799-2116-4, pp: 1-6.

Kim, J.L. and K.D. Kim, 2016. Presentation of central motion techniques: Limpness motion function and limpness sensory unit function. Intl. J. Adv. Culture Technol., 4: 56-61.

Kim, J.L. and K.D. Kim, 2017. Prediction of shiver differentiation by the form alteration on the stable condition. Intl. J. Internet Broadcast. Commun., 9: 8-13.

Kim, J.L. and K.S. Hwang, 2015. Study of quake wavelength of dynamic movement with posture. Intl. J. Adv. Smart Convergence, 4: 99-103.

Kim, J.L., J.S. Choi and K.S. Hwang, 2017. A study on anticipation system of shudder distinction by the physical shape alteration in static condition. J. Inst. Internet Broadcast. Commun., 17: 115-120.

Lopez, Y.A., M.E.D.C. Gomez and F.L.H. Andres, 2017. A received signal strength RFID-based indoor location system. Sens. Actuators A Phys., 255: 118-133.

Nikkhoo, A., F.R. Rofooei and M.R. Shadnam, 2007. Dynamic behavior and modal control of beams under moving mass. J. Sound Vib., 306: 712-724.

Rofooei, F.R., A. Enshaeian and A. Nikkhoo, 2017. Dynamic response of geometrically nonlinear, elastic rectangular plates under a moving mass loading by inclusion of all inertial components. J. Sound Vib., 394: 497-514.

Zhang, J., G.Y. Tian and A.B. Zhao, 2017. Passive RFID sensor systems for crack detection and characterization. NDT. E. Intl., 86: 89-99.